# Similarity-assisted Variational Autoencoder for Nonlinear Dimension Reduction with Application to Single-cell RNA Sequencing Data

Gwangwoo Kim and Hyonho Chun

Department of Mathematical Sciences
Korea Advanced Institute of Science and Technology

# Outline

1 Introduction

2 Preliminary

3 Method

4 Experiment

5 Conclusion

# Introduction

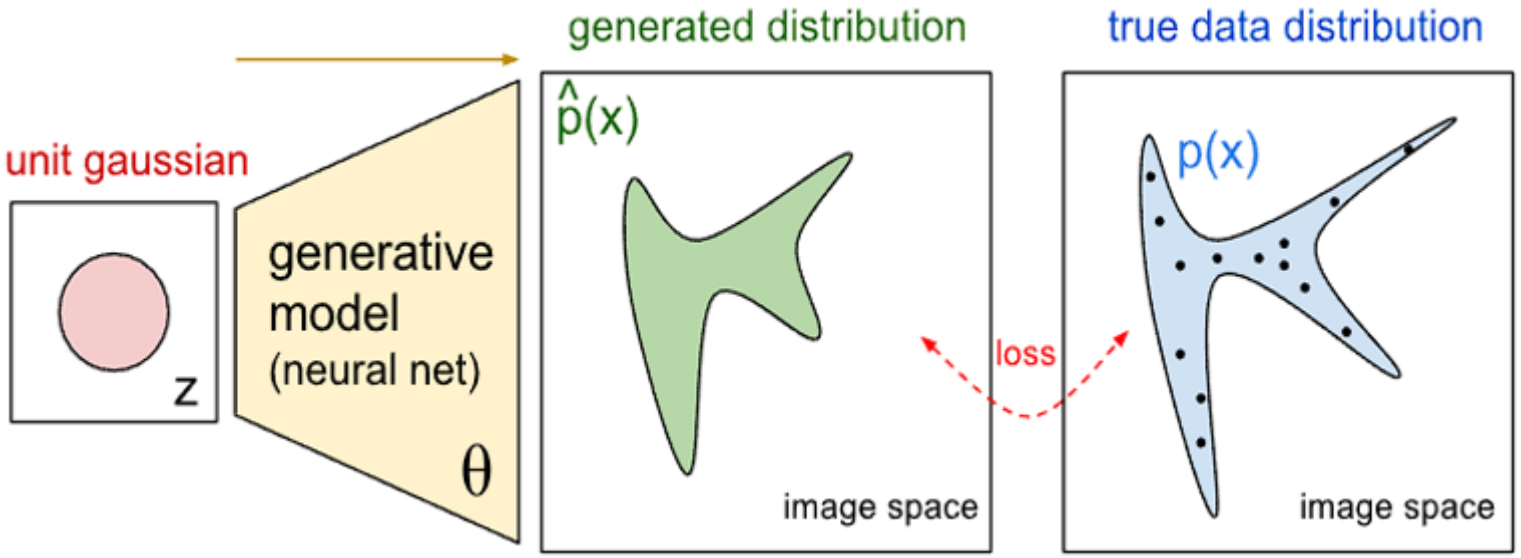


Figure: The generative modeling process

- A generative model describes how a dataset is generated.

# Introduction

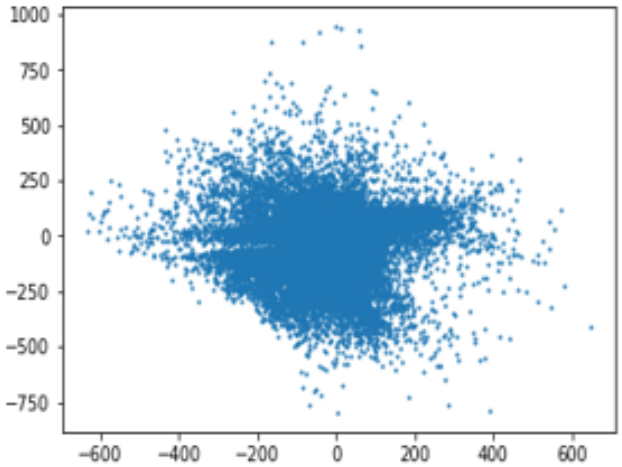


(a) Latent space without true labels

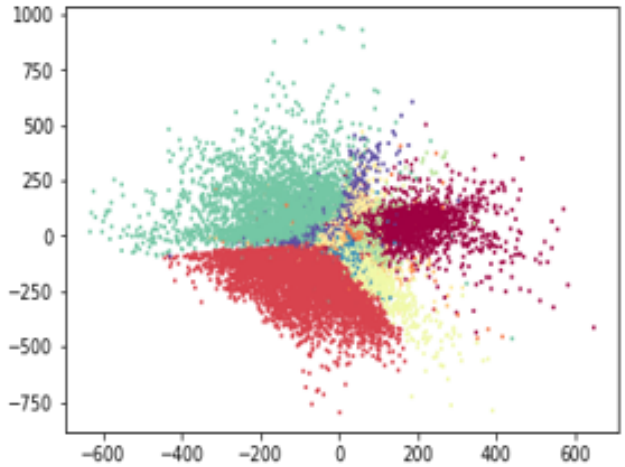


(b) Latent space without true labels

Figure: The latent encoding of the MNIST data from variational autoencoder (VAE)

- The inferred space is hard to interpret without further information.

# Introduction

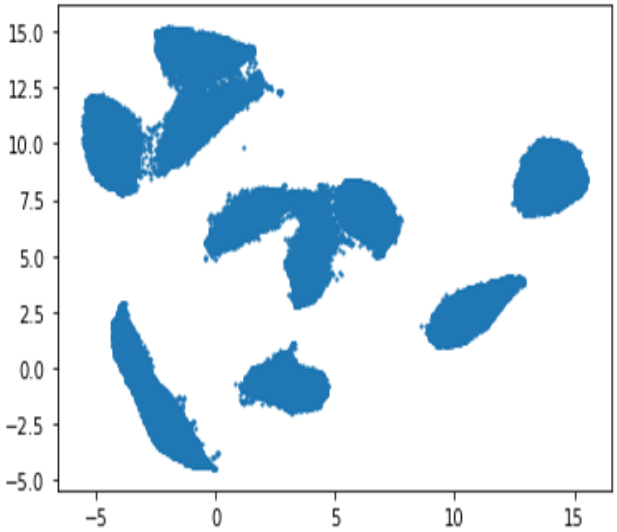


(a) Latent space without true labels

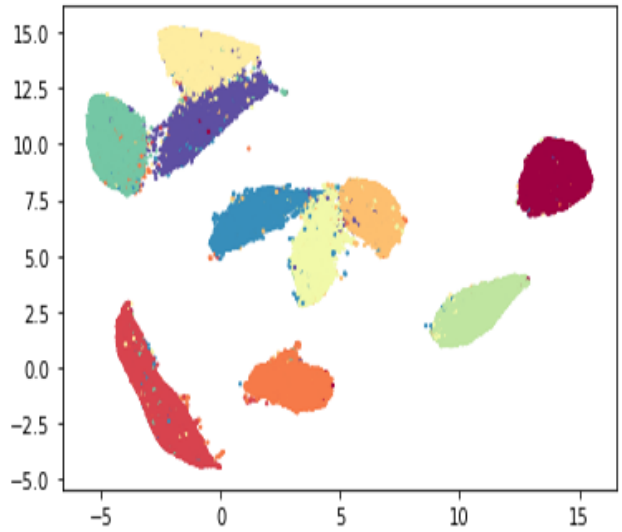


(b) Latent space without true labels

Figure: The visualization of the same data from a dimension reduction method

- Incorporate the similarity information to better illustrate the latent structure.

# Introduction

## Deep generative models

- **Variational autoencoder (VAE)**
- Generative adversarial networks (GAN)
- Flow-based generative model

## Dimension Reduction Algorithms

- **Uniform manifold approximation and projection (UMAP)**
- t-distributed stochastic neighbor embedding (t-SNE)
- Large-scale Dimensionality Reduction Using Triplets (TriMAP)

# Outline

1 Introduction

2 Preliminary

3 Method

4 Experiment

5 Conclusion

# Preliminary

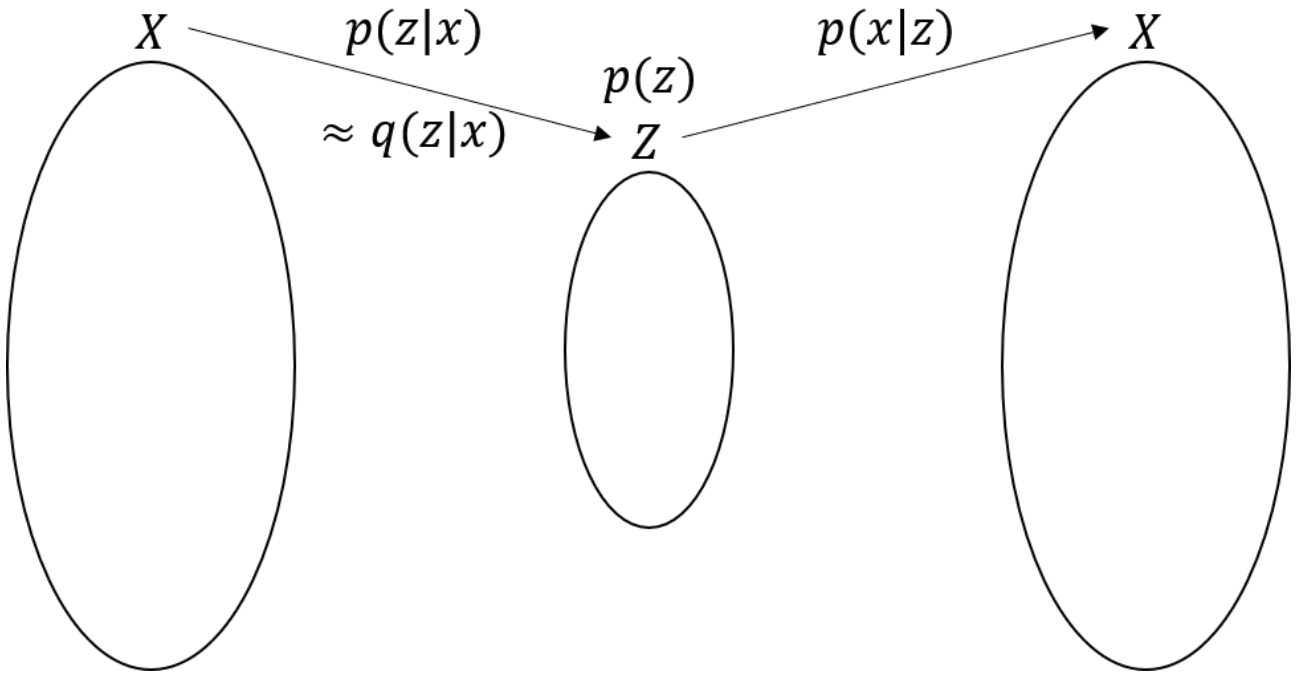


Figure: Variational autoencoder (VAE)

- VAE (Kingma and Welling, 2014) are generative models that attempt to describe data generation through a probabilistic distribution.

## Evidence Lower Bound (ELBO)

The evidence lower bound (ELBO) is an useful lower bound on the log-likelihood of some observed data.

$$\mathbb{E}_{q_\phi(z|x)} \log \frac{p_\theta(z,x)}{q_\phi(z|x)} \leq \log p_\theta(x)$$

## Remark

The ELBO can be decomposed into two components:

$$\begin{aligned}\mathbb{E}_{q_\phi(z|x)} \log \frac{p_\theta(z,x)}{q_\phi(z|x)} &= \mathbb{E}_{q_\phi(z|x)} \log p_\theta(x|z) - \mathbb{E}_{q_\phi(z|x)} \log \frac{q_\phi(z|x)}{p_\theta(z)} \\ &= \mathbb{E}_{q_\phi(z|x)} \log p_\theta(x|z) - D_{\mathrm{KL}}(q_\phi(z|x) \parallel p_\theta(z)).\end{aligned}$$

# Preliminary

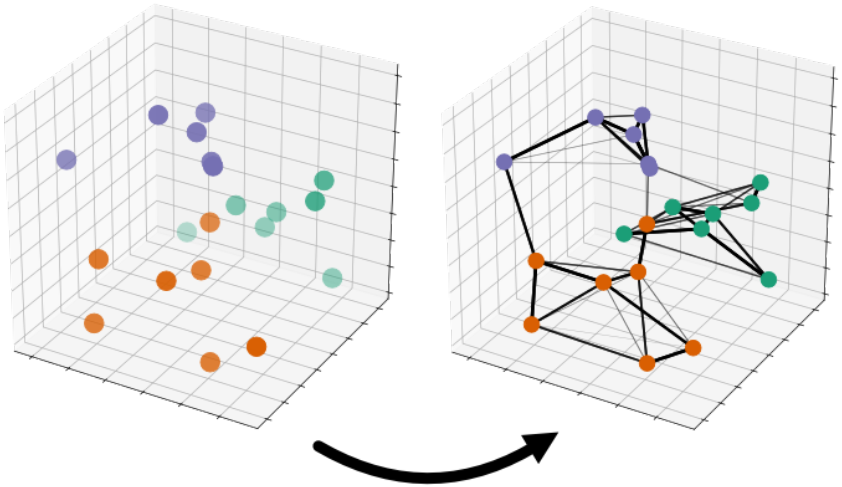


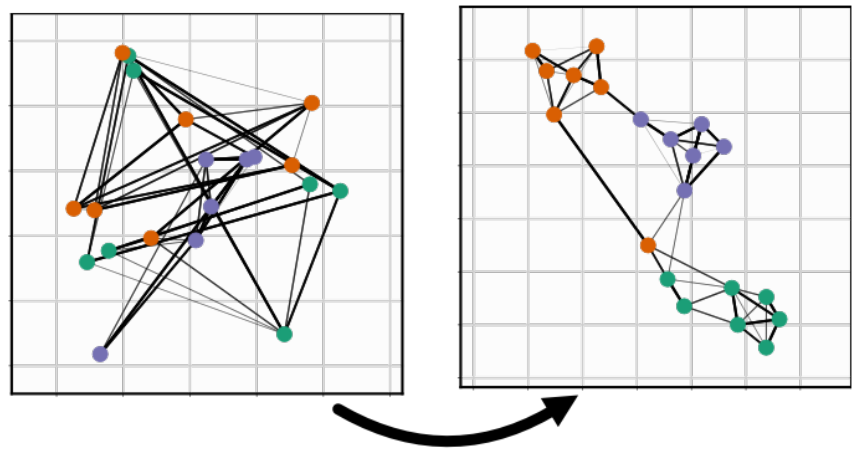


- Uniform manifold approximation and projection (McInnes et al., 2018) is an algorithm for dimension reduction based on manifold learning techniques.

## Graph construction

1. For an observation $x_i$, denote the $k$-nearest neighborhoods by $\{x_{i_j}\}_{j=1}^{k}$. Define the weight function by

$$w(x_i, x_j) = \begin{cases} \exp(\frac{-\max(0, d(x_i, x_j) - \rho_i)}{\sigma_i}) & \text{for } j \in \{i_1, ..., i_k\} \\ 0 & \text{otherwise,} \end{cases}$$

   where $\rho_i$ is the minimum positive distance from $x_i$ and $\sigma_i$ is a normalizing constant.

2. The symmetrized similarity can be computed as

$$\mu_{ij} = w(x_i, x_j) + w(x_j, x_i) - w(x_i, x_j)w(x_j, x_i).$$

## Layout optimization

1. Let $y_i$ be an initial embedding of $x_i$.
2. The similarities among the embeddings are approximations to $\mu_{ij}$, which can be defined as

$$\nu_{ij} := \frac{1}{1 + a\|y_i - y_j\|^{2b}},$$

   where $a$ and $b$ are pre-defined numbers.
3. Optimize the cross entropy loss of $\mu_{ij}$ and $\nu_{ij}$, i.e.,

$$-\sum_i \sum_{j \neq i} \mu_{ij} \ln(\nu_{ij}) + (1 - \mu_{ij}) \ln(1 - \nu_{ij}).$$

# Outline

1 Introduction

2 Preliminary

3 Method

4 Experiment

5 Conclusion

# Method

## Contributions

There are three big deals to integrate the mentioned algorithms.

- Their optimization targets are different.
- Their batch schemes conflict each other.
- It is difficult to strike a balance between them.

# Method

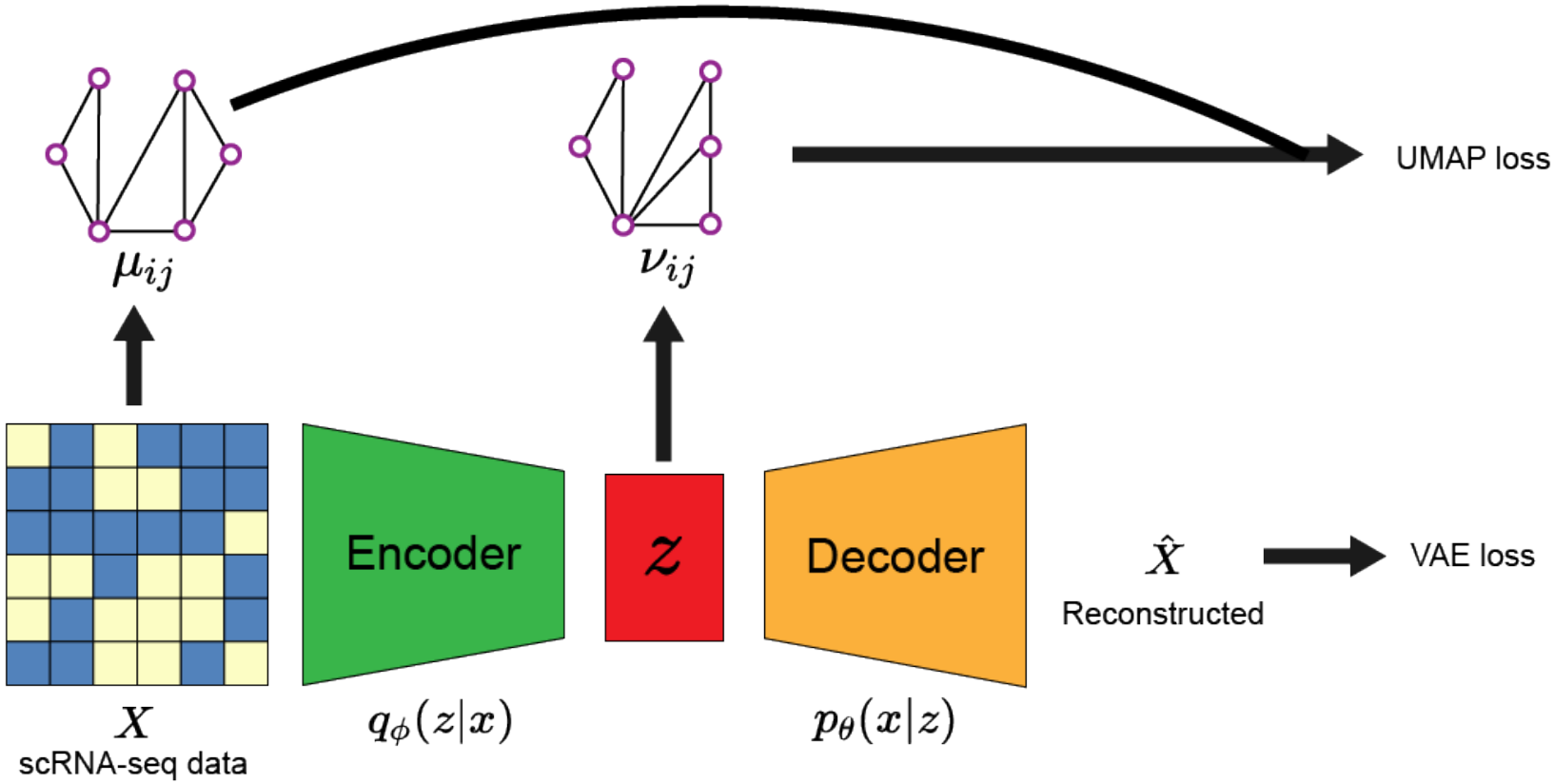


Figure: Overview of saVAE

- Our saVAE connects the VAE and UMAP objective functions by utilizing the expected UMAP loss function,

# Method

## saVAE

Similarity-assisted VAE (saVAE) unifies VAE and UMAP, and its objective function is given by

$$-(\text{ELBO}) - \lambda \sum_i \sum_{j \neq i} \mu_{ij} \ln(\tilde{\nu}_{ij}) + (1 - \mu_{ij}) \ln(1 - \tilde{\nu}_{ij}),$$

where $\tilde{\nu}_{ij} = \left[ \mathbb{E}_{q_\phi(z|x_i)} \mathbb{E}_{q_\phi(z'|x_j)} \frac{1}{1 + a\|z - z'\|^{2b}} \right]$ and $\lambda$ is a weight.

# Method

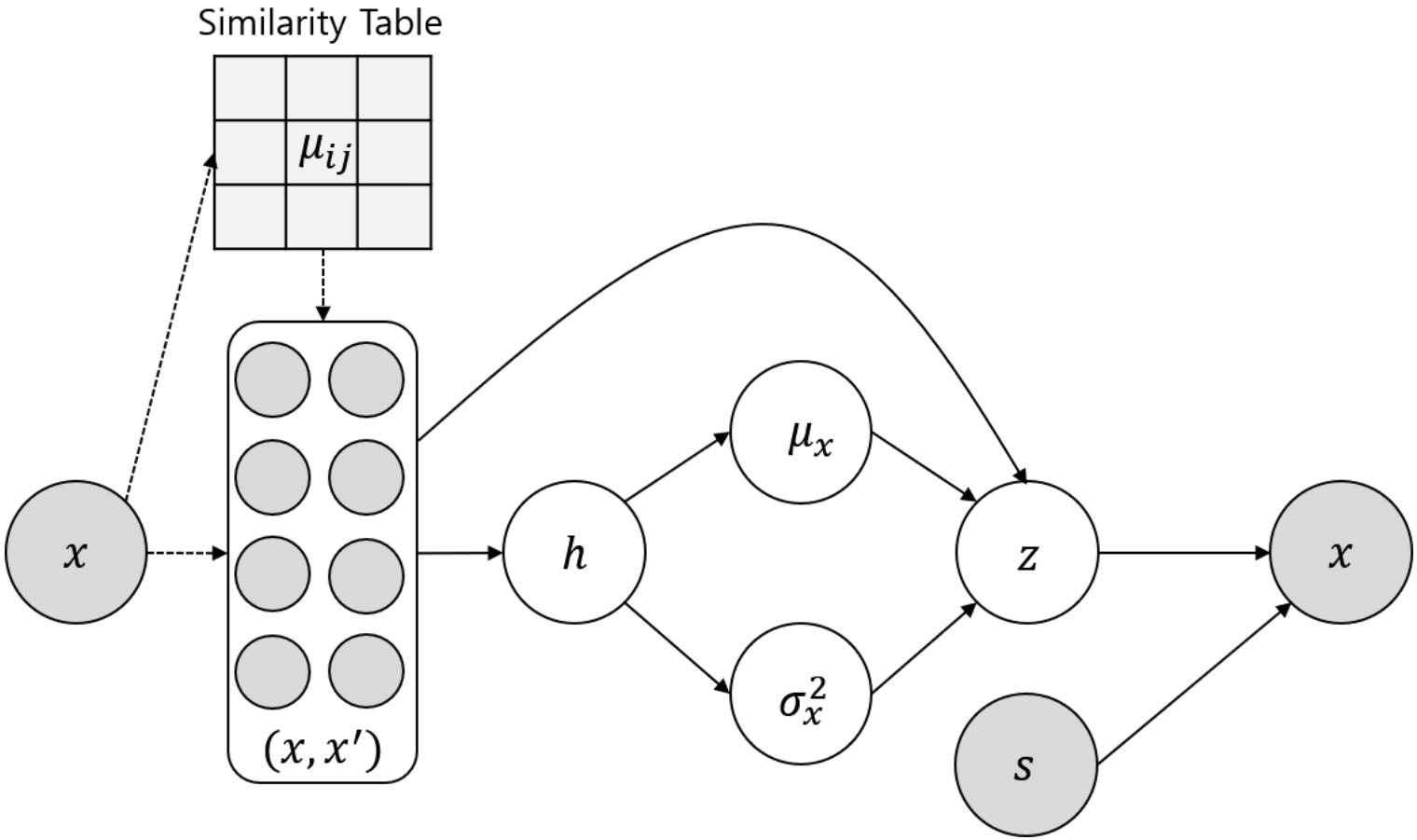


Figure: Graphical model of our saVAE

# Method

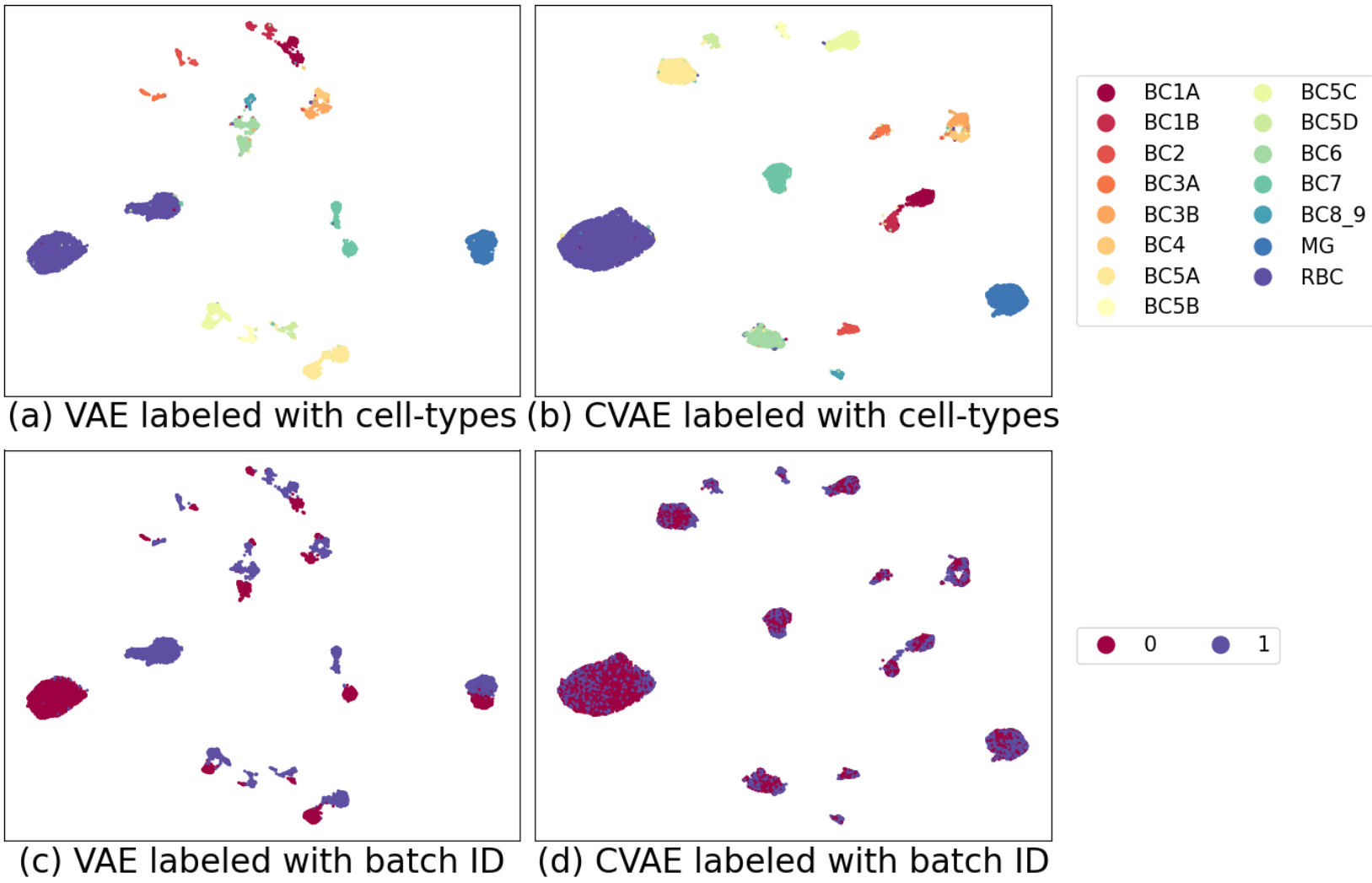


(a) VAE labeled with cell-types (b) CVAE labeled with cell-types

(c) VAE labeled with batch ID (d) CVAE labeled with batch ID

Figure: Embeddings from retina dataset

# Method

## saCVAE

For additional information $s$, our objective function of the saCVAE is

$$-\mathbb{E}_{q_\phi(z|x)} \log p_\theta(x|z, s) + \mathbb{E}_{q_\phi(z|x)} \log \frac{q_\phi(z|x)}{p_\theta(z)}$$
$$-\lambda \sum_i \sum_{j \neq i} \tilde{\mu}_{ij} \ln(\tilde{\nu}_{ij}) + (1 - \tilde{\mu}_{ij}) \ln(1 - \tilde{\nu}_{ij}),$$

where $\tilde{\mu}_{ij}$ is the weight computed from the covariate-adjusted embeddings and $\tilde{\nu}_{ij}$ and $\lambda$ are defined in the previous section.

# Outline

1 Introduction

2 Preliminary

3 Method

4 Experiment

5 Conclusion

# Experiment

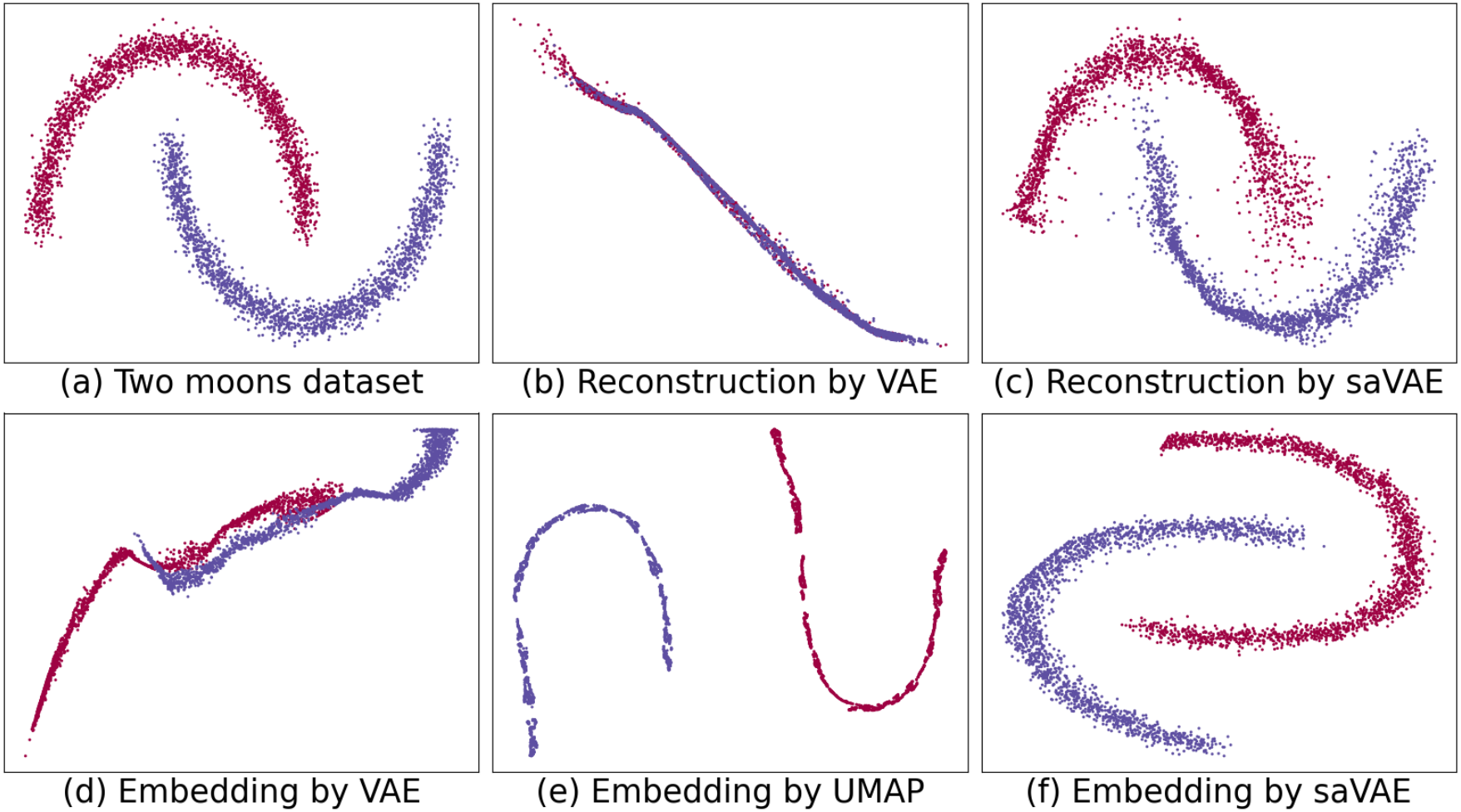


Figure: Method comparison using two moons dataset

# Experiment

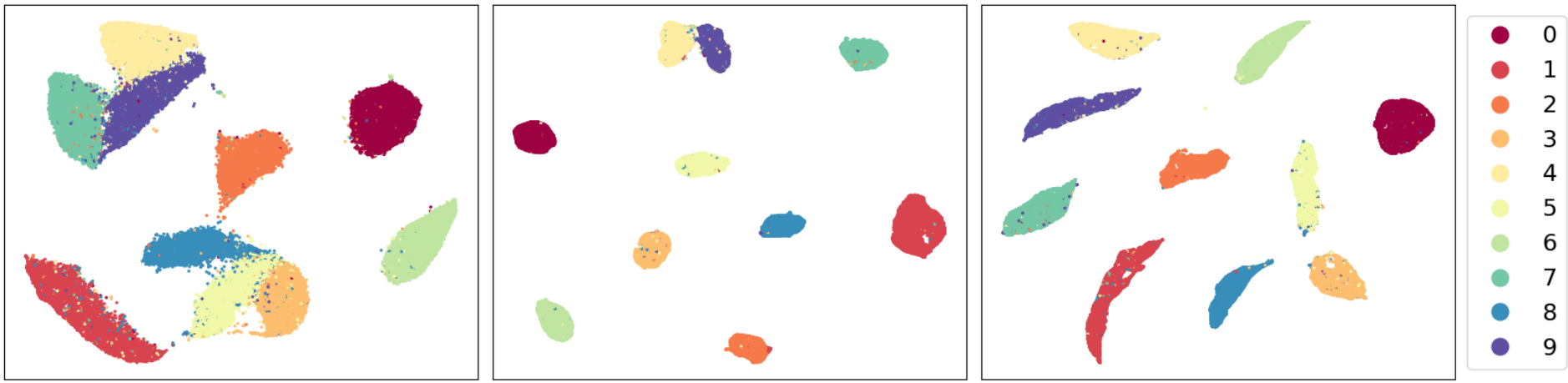


(a) UMAP (b) DGG (c) saVAE

Figure: Embeddings from MNIST dataset, which is a set of handwritten digits images from 0 to 9.

# Experiment

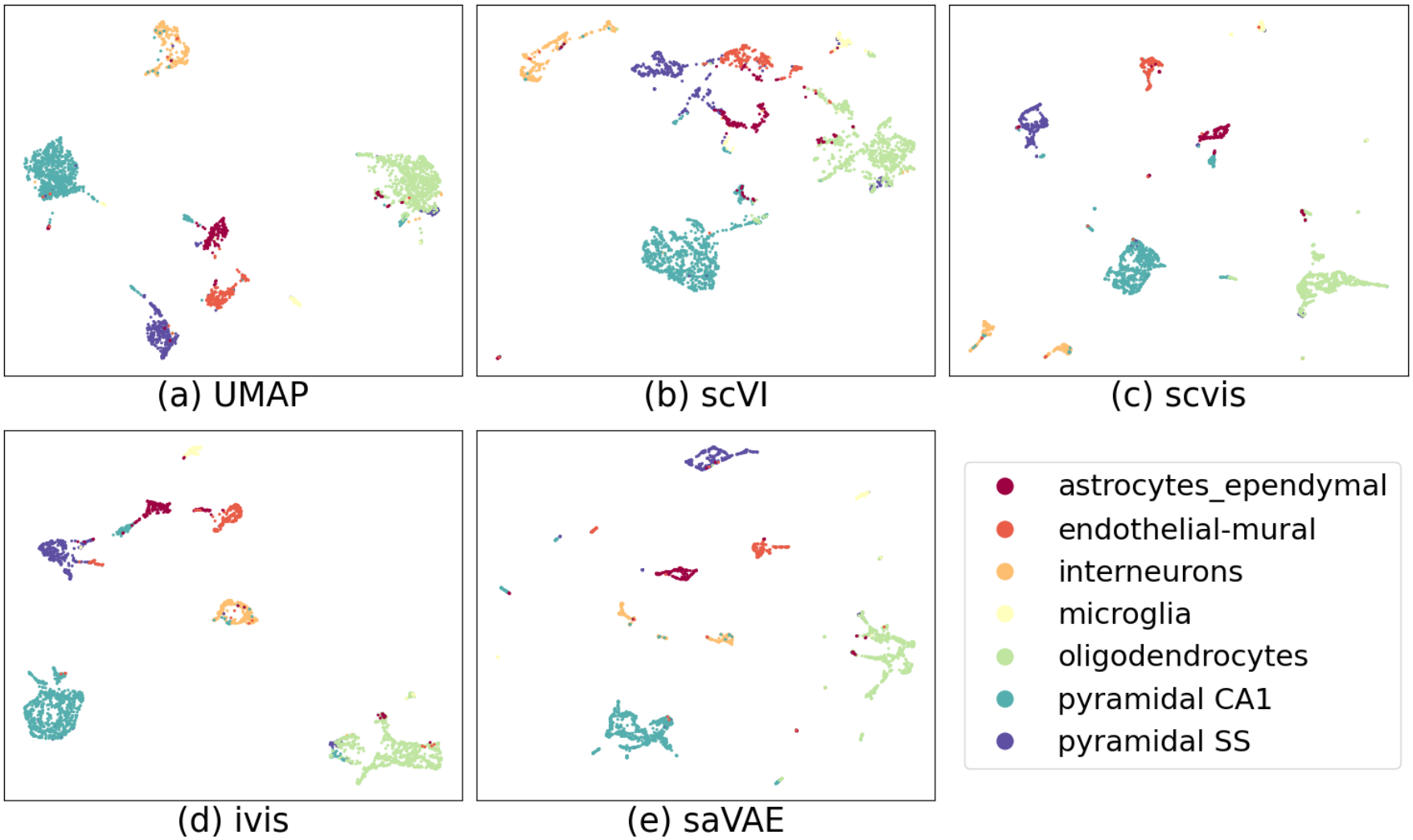


Figure: Embeddings from cortex dataset

# Experiment

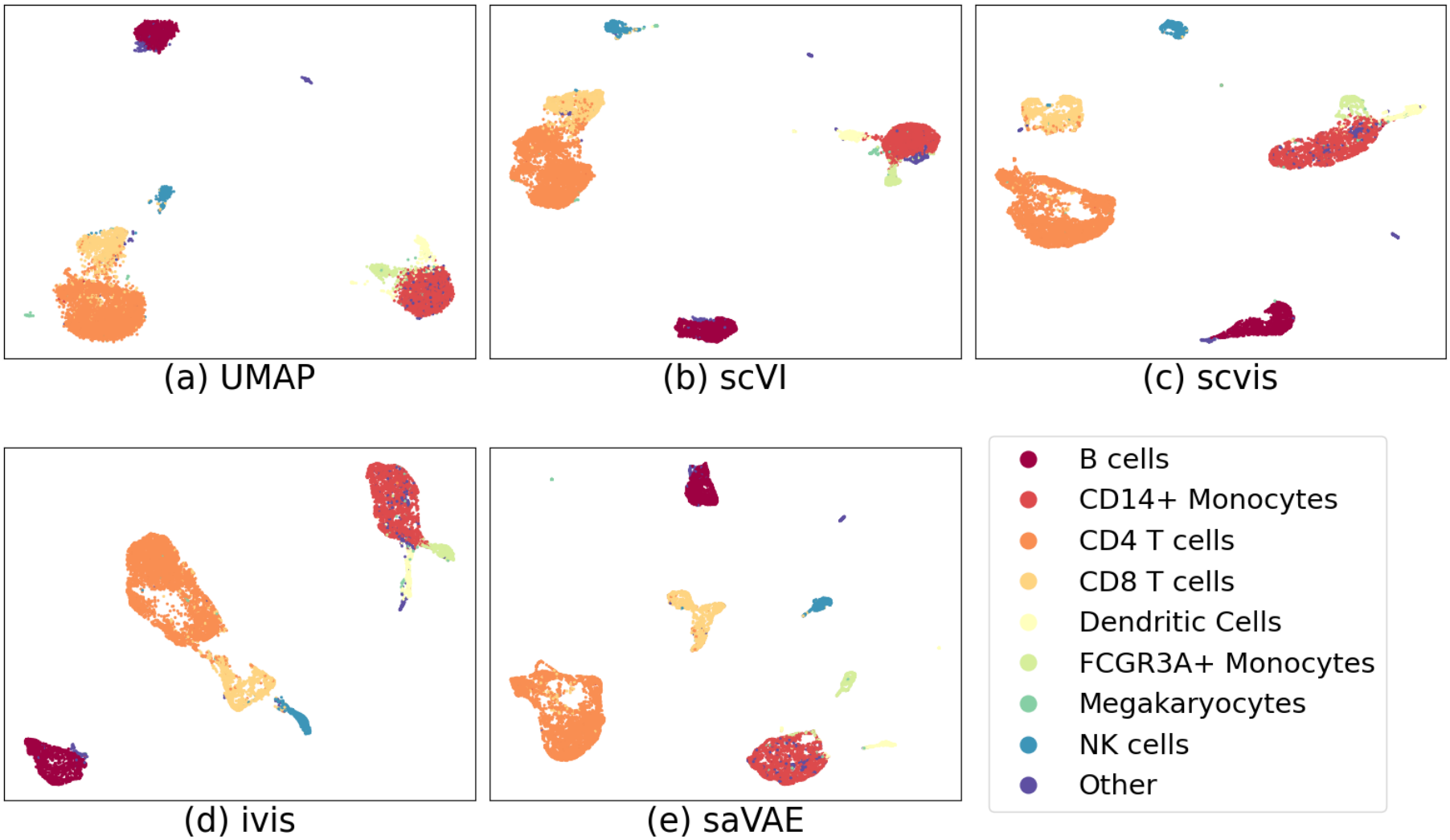


Figure: Embeddings from PBMC dataset

# Experiment

| Dataset | Method | ARI | NMI | Dataset | Method | ARI | NMI |
|---|---|---|---|---|---|---|---|
| cortex | UMAP | 0.79 | **0.78** | PBMC | UMAP | **0.84** | 0.80 |
| | scvis | 0.79 | 0.77 | | scvis | 0.82 | 0.79 |
| | Ivis | 0.70 | 0.72 | | Ivis | 0.63 | 0.69 |
| | scVI | 0.75 | 0.72 | | scVI | 0.53 | 0.72 |
| | saVAE | **0.80** | 0.77 | | saVAE | **0.84** | **0.81** |

Table: Performance comparison. Our saVAE performs better than UMAP, scvis, Ivis, and scVI. All values are reported as the highest out of 10 trials.

# Experiment

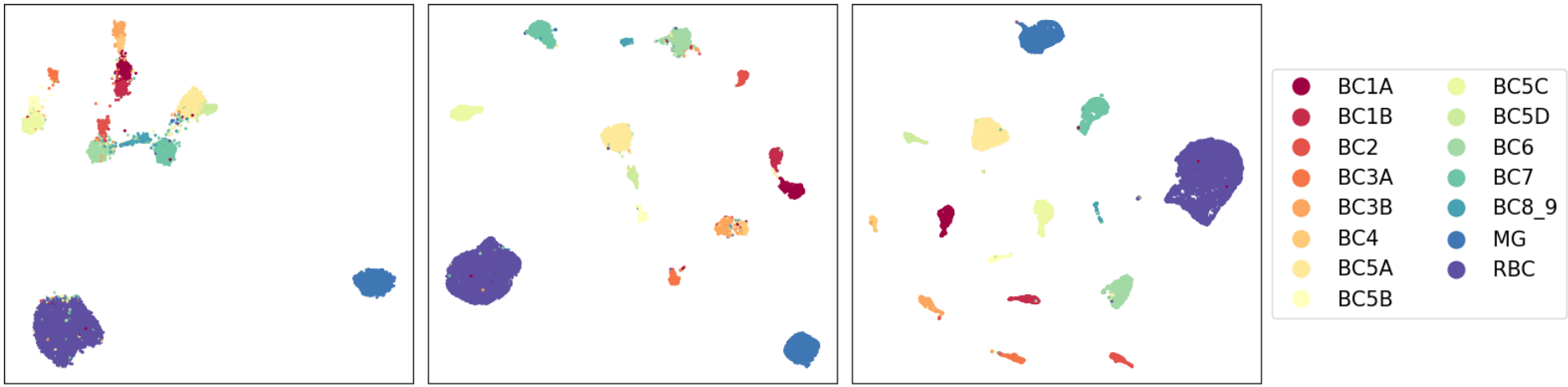


(a) UMAP (b) scVI (c) saCVAE

Figure: Embeddings from retina dataset

# Experiment

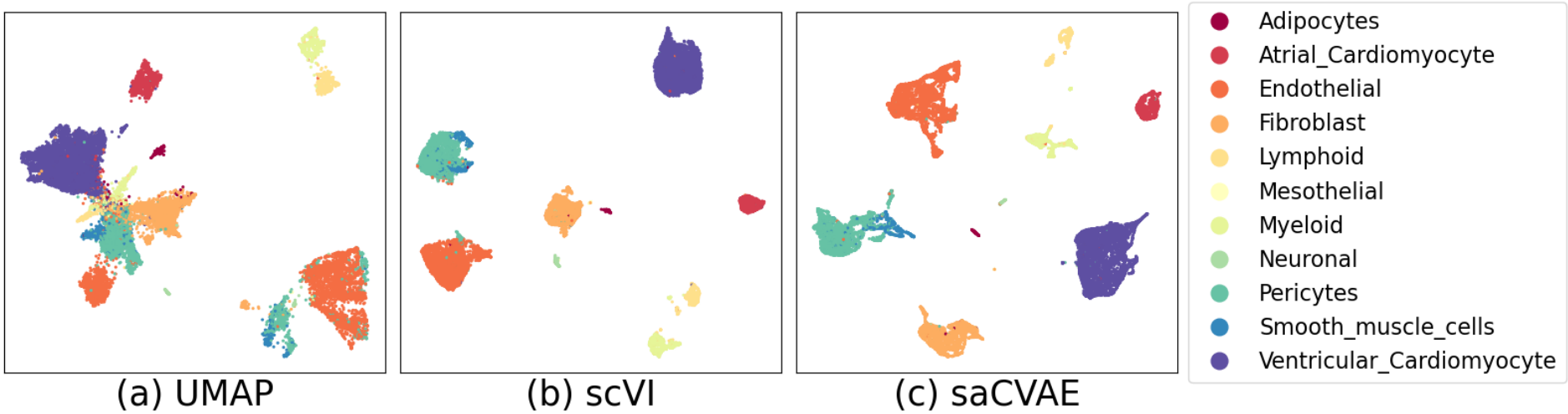


Figure: Embeddings from heart cell atlas dataset

# Experiment

| Dataset | Method | ARI | NMI | Dataset | Method | ARI | NMI |
|---|---|---|---|---|---|---|---|
| retina | UMAP | 0.90 | 0.85 | heart cell atlas | UMAP | 0.64 | 0.69 |
| | scVI | 0.56 | 0.84 | | scVI | 0.72 | 0.80 |
| | saVAE | **0.98** | **0.95** | | saVAE | **0.93** | **0.92** |

Table: Performance comparison. Our saCVAE formulation effectively eliminates the covariate effects, resulting in a better cell-type clustering performance. All values are reported as the highest out of 10 trials.

# Outline

1 Introduction

2 Preliminary

3 Method

4 Experiment

5 Conclusion

# Conclusion

## Conclusions

- We propose a framework to combine VAE based and similarity based approaches to reflect intrinsic structures in the data.
- Computational conflicts are resolved via applying a sampling idea to a normal mini-batch.
- By introducing CVAE, it is possible to adjust the covariate effect of transcriptomes, with one framework.

# References

Diederik P. Kingma and Max Welling. Auto-Encoding Variational Bayes. In Yoshua Bengio and Yann LeCun, editors, *2nd International Conference on Learning Representations, ICLR 2014, Banff, AB, Canada, April 14-16, 2014, Conference Track Proceedings*, 2014.

Leland McInnes, John Healy, Nathaniel Saul, and Lukas Grossberger. UMAP: Uniform Manifold Approximation and Projection. *The Journal of Open Source Software*, 3:861, 2018.